

# Lecture 9: Compressible Aerodynamics

## Aerodynamics

Aniruddha Sinha

*Department of Aerospace Engineering, IIT Bombay*

November 4, 2022

Given the success of potential flow theory in incompressible aerodynamics, the overall motivation here is to try to extend the same tools to the compressible flow over airfoils and wings. It turns out that for thin airfoils, compressibility effects can be accounted for by applying very simple ‘correction factors’ to the corresponding incompressible potential flow results. This is of immense utility – instead of performing experiments over a range of Mach numbers, one can do a single test at a very low speed (incompressible flow regime), and then readily extend this result to a large range of *subsonic* freestream speeds. We will prove this contention in this lecture.

The above simplification is applicable in shock-free flows. Thus, we first study in figure 1 how shocks appear in flow over airfoils as the freestream Mach number is increased. For the particular representative airfoil depicted (at a particular angle of attack), the entire flow is shock-free up to  $M_\infty = 0.58$ . At this speed, the flow is accelerated over the suction surface to just reach sonic condition at a particular point, before decelerating again. This Mach

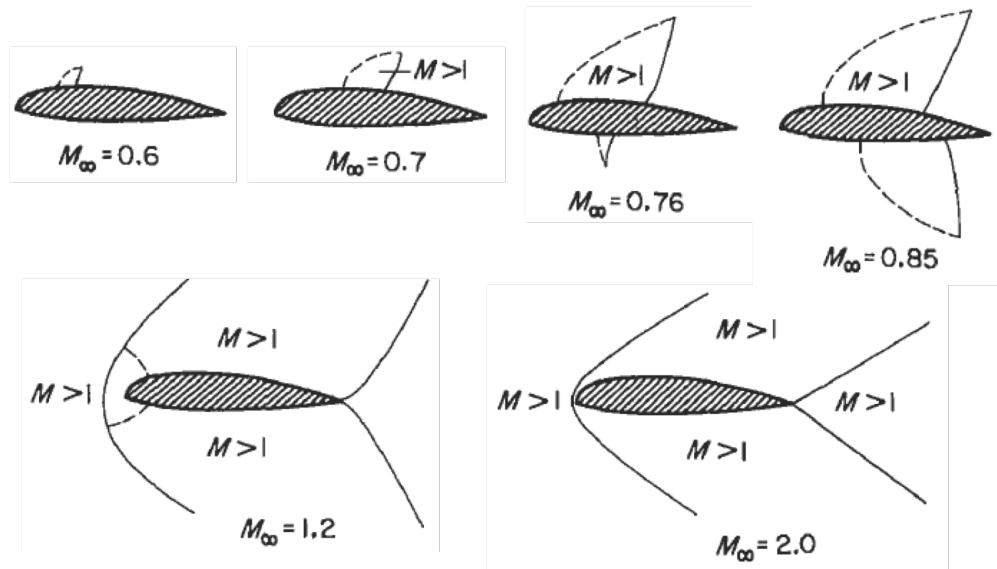


Figure 1: Flow development on 2D airfoil with increasing  $M_\infty$  [Houghton et al., 2013]

number is called the critical Mach number,  $M_{cr}$ , for the airfoil at the particular  $\alpha$ .

If  $M_\infty$  is increased beyond the critical value, a small pocket of supersonic flow appears on the suction surface as shown, and it is terminated by a (weak) shock so that the flow is subsonic everywhere else. The pocket of supersonic flow increases in size (and strength) as the  $M_\infty$  increases; a similar pocket also appears on the pressure side. Note that the terminating shock moves aft on both surfaces of the airfoil with increasing subsonic  $M_\infty$ .

The flow is fundamentally different if the freestream is supersonic. At low supersonic speeds, a bow shock forms near the leading edge, which has a small pocket of subsonic flow just behind it. The remainder of the flow over both surfaces of the airfoil is supersonic (since the bow shock is predominantly oblique), but the Mach number is less than that of the freestream. As the freestream Mach number increases, the bow shock starts to resemble two oblique shocks, with the subsonic pocket getting compacted more and more. At the trailing edge, we have an oblique shock on the suction side; the pressure side can have a shock or an expansion fan depending on the geometry and angle of attack.

## 1 Full potential equation for compressible flows

In this section, we follow Anderson [2011].

We now derive the governing equation(s) for inviscid, irrotational, steady, compressible flow in Cartesian coordinates. Note that these equations do not account for the special nature of airfoil flow. It will turn out that these equations are too complicated for analytical solution, and we most often resort to simplifications.

As in the case of incompressible flow, owing to irrotationality, the (compressible) velocity field  $\underline{V}$  is associated with a ‘full’ velocity potential  $\Phi$  (the reason for this nomenclature will be clear subsequently)

$$\underline{V} =: \nabla \Phi.$$

In Cartesian coordinates, we have

$$U = \frac{\partial \Phi}{\partial x} =: \Phi_x, \quad V = \frac{\partial \Phi}{\partial y} =: \Phi_y, \quad W = \frac{\partial \Phi}{\partial z} =: \Phi_z,$$

where the subscript denotes differentiation with respect to the indicated variable. For later reference, we will denote  $\partial^2 \Phi / \partial x \partial y$  as  $\Phi_{xy}$ , etc. Note that, for notational convenience, we denote ‘full’ quantities by upper case symbols, although we have typically used lower case symbols for the same earlier. This is because we wish to reserve the corresponding lower case symbols for the ‘perturbation’ quantities to follow.

Substituting this in the steady mass conservation equation, we have

$$\nabla \cdot (\rho \underline{V}) = \rho (\Phi_{xx} + \Phi_{yy} + \Phi_{zz}) + \Phi_x \rho_x + \Phi_y \rho_y + \Phi_z \rho_z = 0. \quad (1)$$

N.B.: In incompressible flow, we would straightaway obtain  $\nabla^2 \Phi = 0$ .

To eliminate density from the above equation, we take recourse to the irrotational form of the momentum conservation equation

$$dp = -\rho d(\|\underline{V}\|^2/2) = -\frac{\rho}{2} d(\Phi_x^2 + \Phi_y^2 + \Phi_z^2). \quad (2)$$

Further, as we are considering inviscid shock-free flow, isentropic flow assumption is valid. In this case, the speed of sound  $a$  is given by  $a = \sqrt{dp/d\rho}$ . Or, rearranging and using eqn (2),

$$d\rho = \frac{dp}{a^2} = -\frac{\rho}{2a^2} d(\Phi_x^2 + \Phi_y^2 + \Phi_z^2).$$

In particular,

$$\rho_x = -\frac{\rho}{a^2} (\Phi_x \Phi_{xx} + \Phi_y \Phi_{yx} + \Phi_z \Phi_{zx}),$$

with similar expressions obtaining for  $\rho_y$  and  $\rho_z$ .

Substituting these in expressions in eqn (1), we have

$$\begin{aligned} & \left(1 - \frac{\Phi_x^2}{a^2}\right) \Phi_{xx} + \left(1 - \frac{\Phi_y^2}{a^2}\right) \Phi_{yy} + \left(1 - \frac{\Phi_z^2}{a^2}\right) \Phi_{zz} \\ & - 2\frac{\Phi_x \Phi_y}{a^2} \Phi_{xy} - 2\frac{\Phi_y \Phi_z}{a^2} \Phi_{yz} - 2\frac{\Phi_z \Phi_x}{a^2} \Phi_{zx} = 0. \end{aligned} \quad (3)$$

In Cartesian tensor notation, this reduces to

$$\Phi_{ii} - \frac{\Phi_i \Phi_j}{a^2} \Phi_{ij} = 0.$$

Note that we do not have a well-posed problem as yet since both  $a$  and  $\Phi$  are variables, and we have just obtained one equation. To make progress, we now resort to the adiabatic energy equation in the absence of molecular diffusive processes (i.e., viscosity and thermal conductivity are neglected), viz.

$$C_p dT + d(\|\underline{V}\|^2/2) = 0.$$

Assuming a perfect gas (for which  $C_p$  is constant), integration of the above yields

$$C_p T + \|\underline{V}\|^2/2 = \text{Constant}. \quad (4)$$

Recalling the definition of total (or stagnation) conditions, we find that the above constant is actually  $C_p T_0$ . Then, using the expression  $C_p = \gamma R/(\gamma - 1)$ , along with the isentropic flow assumption to write  $a = \sqrt{\gamma RT}$ , we obtain

$$a = \sqrt{a_0^2 - (\gamma - 1)(\Phi_x^2 + \Phi_y^2 + \Phi_z^2)/2} = \sqrt{a_0^2 - (\gamma - 1)\Phi_{ii}/2}, \quad (5)$$

where  $a_0 := \sqrt{\gamma RT_0}$ ; the last expression is of course in Cartesian tensor notation.

Substituting  $a$  from eqn (5) in eqn (3), we finally obtain a single (albeit nonlinear) PDE for the compressible velocity potential, instead of five separate PDEs.

This is the ‘full’ potential equation. It may be solved analytically in only a very few special cases to obtain theoretical results. Numerical solution is of course possible, but not as much insight can be derived therefrom. To obtain approximate analytical results for a much wider variety of aerodynamic problems, we have to linearize this.

## 2 Perturbation potential equation

In this section, we follow Anderson [2011].

The full potential equation was derived without leveraging the possible simplicity of (compressible) flow over a slender streamlined airfoil. In particular, we wish to ameliorate the nonlinearity in the full potential equation by expanding the velocity potential as a Taylor series around a suitable ‘base flow’ potential, and subsequently omitting the higher-order terms. For this to be successful, the base flow must be chosen appropriately. The freestream flow is especially simple, and applies to the majority of the flow domain. Thus we may fruitfully consider the actual airfoil flow to be a ‘small’ perturbation of the freestream flow. (It will be noticed that, in this regard, the problem setup is similar to incompressible thin airfoil theory.)

To simplify the notation, we restrict the treatment to two dimensional flow (i.e., flow over an airfoil, and not a wing), although the final equation can be readily extended to 3D. Moreover, we align the  $x$ -axis with the freestream flow. Thus, the perturbation velocity potential  $\phi$  is defined such that

$$\Phi =: V_\infty x + \phi,$$

where  $V_\infty$  is the freestream velocity. Moreover, we have

$$\Phi_x = U = V_\infty + u = V_\infty + \phi_x, \quad \Phi_z = W = w = \phi_z.$$

We will first derive the perturbation potential equation for perturbations that are not necessarily small (i.e., no additional assumptions over those made in obtaining the full potential equations). This would then guide us to the physical conditions under which linearization of the perturbation potential equation will be warranted.

In eqn (5), the energy conservation equation was expressed in terms of the stagnation condition; this was preferred for generality. However, now that we are specializing to flows over airfoils, a more appropriate expression is in terms of the freestream condition:

$$a^2 + \frac{\gamma - 1}{2} (U^2 + W^2) = a_\infty^2 + \frac{\gamma - 1}{2} V_\infty^2.$$

Noting that  $M_\infty = V_\infty/a_\infty$ , and using the perturbation forms of the velocity components, this simplifies as

$$\begin{aligned} \frac{a^2}{a_\infty^2} &= 1 - \frac{\gamma - 1}{2} \left[ \left( M_\infty + \frac{u}{a_\infty} \right)^2 + \left( \frac{w}{a_\infty} \right)^2 - M_\infty^2 \right] \\ &= 1 - \frac{\gamma - 1}{2} M_\infty^2 \left[ \left( 1 + \frac{u}{V_\infty} \right)^2 + \left( \frac{w}{V_\infty} \right)^2 - 1 \right] = 1 - \frac{\gamma - 1}{2} M_\infty^2 \left[ 2 \frac{u}{V_\infty} + \frac{u^2 + w^2}{V_\infty^2} \right]. \end{aligned}$$

A term of interest in the full potential equation (i.e. eqn (3)) is  $a^2 - \Phi_x^2$ . This is now expressed as

$$a^2 - \Phi_x^2 = a^2 - (V_\infty + u)^2 = a_\infty^2 \left[ \frac{a^2}{a_\infty^2} - M_\infty^2 \left\{ 1 + 2 \frac{u}{V_\infty} + \frac{u^2}{V_\infty^2} \right\} \right]$$

$$= a_\infty^2 \left[ 1 - M_\infty^2 - M_\infty^2 \left\{ (\gamma + 1) \frac{u}{V_\infty} + \frac{\gamma + 1}{2} \frac{u^2}{V_\infty^2} + \frac{\gamma - 1}{2} \frac{w^2}{V_\infty^2} \right\} \right].$$

Also,

$$\begin{aligned} a^2 - \Phi_z^2 &= a^2 - w^2 = a_\infty^2 \left[ \frac{a^2}{a_\infty^2} - M_\infty^2 \left\{ \frac{w^2}{V_\infty^2} \right\} \right] \\ &= a_\infty^2 \left[ 1 - M_\infty^2 \left\{ (\gamma - 1) \frac{u}{V_\infty} + \frac{\gamma - 1}{2} \frac{u^2}{V_\infty^2} + \frac{\gamma + 1}{2} \frac{w^2}{V_\infty^2} \right\} \right]. \end{aligned}$$

The other term of interest for simplifying eqn (3) is  $\Phi_x \Phi_z$ ; this is written as

$$\Phi_x \Phi_z = (V_\infty + u) w = a_\infty^2 M_\infty^2 \left( 1 + \frac{u}{V_\infty} \right) \frac{w}{V_\infty}.$$

Thus, the 2D potential equation in terms of (not necessarily small) perturbations (i.e. without additional assumptions) is

$$\begin{aligned} (1 - M_\infty^2) \frac{\partial u}{\partial x} + \frac{\partial w}{\partial z} &= M_\infty^2 \left\{ (\gamma + 1) \frac{u}{V_\infty} + \frac{\gamma + 1}{2} \frac{u^2}{V_\infty^2} + \frac{\gamma - 1}{2} \frac{w^2}{V_\infty^2} \right\} \frac{\partial u}{\partial x} \\ &\quad + M_\infty^2 \left\{ (\gamma - 1) \frac{u}{V_\infty} + \frac{\gamma - 1}{2} \frac{u^2}{V_\infty^2} + \frac{\gamma + 1}{2} \frac{w^2}{V_\infty^2} \right\} \frac{\partial w}{\partial z} \\ &\quad + 2M_\infty^2 \left\{ \frac{w}{V_\infty} + \frac{uw}{V_\infty^2} \right\} \frac{\partial u}{\partial z}. \end{aligned} \quad (6)$$

The LHS is linear in perturbations, whereas the RHS is nonlinear. If  $M_\infty$  is small (low subsonic), then  $\text{RHS} = 0$ , and the LHS reduces to the Laplacian of the perturbation potential  $\phi$ . Thus,  $\partial u / \partial x + \partial w / \partial z = 0$  governs the perturbations, even if they are not particularly small (i.e. even if  $u/V_\infty$  and  $w/V_\infty$  are not necessarily small). This is the case of incompressible flow over a (possibly thick) airfoil, as treated extensively earlier, for which the Laplace equation governs the full and perturbation potential.

In case  $M_\infty$  is *not* small (i.e., flow is compressible), *partial* linearization may be achieved if  $u/V_\infty \ll 1$  and  $w/V_\infty \ll 1$ ; this is the case of a thin airfoil at a low angle of attack. Under this assumption, we can neglect the higher order terms in the braces in eqn (6) to obtain

$$(1 - M_\infty^2) \left\{ 1 - (\gamma + 1) \frac{M_\infty^2}{1 - M_\infty^2} \frac{u}{V_\infty} \right\} \frac{\partial u}{\partial x} + \left\{ 1 - (\gamma - 1) M_\infty^2 \frac{u}{V_\infty} \right\} \frac{\partial w}{\partial z} - \left\{ 2M_\infty^2 \frac{w}{V_\infty} \right\} \frac{\partial u}{\partial z} \approx 0.$$

Assuming that the derivatives of the two components of perturbation velocity are of similar order, *full* linearization will be achieved if (recalling the assumptions already made)

$$\frac{u}{V_\infty}, \frac{w}{V_\infty} \ll 1 \quad \text{and} \quad \frac{M_\infty^2}{1 - M_\infty^2} \frac{u}{V_\infty} \ll 1 \quad \text{and} \quad M_\infty^2 \frac{u}{V_\infty}, M_\infty^2 \frac{w}{V_\infty} \ll 1. \quad (7)$$

As mentioned earlier, the first condition holds for thin airfoils at low angles of attack. Additionally, for linearization, the second condition (in concert with the first) states that  $M_\infty$

must not be very close to sonic. The last condition, in association with the first, requires that  $M_\infty$  must not be very large, i.e., low supersonic freestream condition is mandated.

In conclusion, the linearized perturbation potential equation is

$$(1 - M_\infty^2) \frac{\partial u}{\partial x} + \frac{\partial w}{\partial z} = 0, \quad (8)$$

and it is valid if, as a rule of thumb,

$$\text{EITHER } M_\infty \ll 1, \text{ even for moderately thick airfoils,} \quad (9a)$$

$$\text{OR } M_\infty \gtrsim 0.8 \text{ or } 1.2 \gtrsim M_\infty \gtrsim 5, \text{ for thin airfoils at low } \alpha. \quad (9b)$$

(Note that eqn (9b) is simply a physical restatement of the mathematical assumptions described by eqn (7).) In other words, the linearized eqn (8) is valid under the usual assumptions of thin airfoil theory, both for low subsonic and moderate supersonic freestream conditions, as long as transonic conditions are avoided.

Before leaving this topic, we note that the three-dimensional version of the linearized perturbation potential equation is directly deduced to be

$$(1 - M_\infty^2) \frac{\partial u}{\partial x} + \frac{\partial v}{\partial y} + \frac{\partial w}{\partial z} = 0. \quad (10)$$

## 2.1 Pressure coefficient for linear perturbations

From its definition,

$$c_p = \frac{p - p_\infty}{0.5 \rho_\infty V_\infty^2} = 2 \left( \frac{p}{p_\infty} - 1 \right) \frac{p_\infty}{\rho_\infty a_\infty^2} \frac{a_\infty^2}{V_\infty^2}.$$

Since  $a_\infty^2 = \gamma p_\infty / \rho_\infty$ , we have the general expression for pressure coefficient in compressible flows (without any assumption)

$$c_p = \frac{2}{\gamma M_\infty^2} \left( \frac{p}{p_\infty} - 1 \right). \quad (11)$$

For isentropic flows,  $p/p_\infty = (T/T_\infty)^{\gamma/(\gamma-1)}$ . Thus, we seek a simplified expression for  $T/T_\infty$ , for which we look to the energy equation (viz. eqn (4)). Specializing the RHS to the freestream condition (and recalling that  $C_p T_\infty = \gamma R T_\infty / (\gamma - 1) = a_\infty^2 / (\gamma - 1)$ ),

$$\begin{aligned} C_p T + \frac{U^2 + W^2}{2} &= C_p T_\infty + \frac{V_\infty^2}{2} \\ \Rightarrow \frac{T}{T_\infty} &= 1 + \frac{1}{2 C_p T_\infty} \{ V_\infty^2 - (V_\infty + u)^2 - w^2 \} = 1 - \frac{\gamma - 1}{2} M_\infty^2 \left\{ \frac{2u}{V_\infty} + \frac{u^2 + w^2}{V_\infty^2} \right\}. \end{aligned}$$

Now specializing to linear perturbations (specifically invoking the first assumption in eqn (7)), whereby the higher-order terms in braces are rendered negligible, we have

$$\frac{T}{T_\infty} \approx 1 - (\gamma - 1) M_\infty^2 \frac{u}{V_\infty}.$$

Recall from the assumptions for linearized perturbations (specifically the third assumption in eqn (7)) that the second term is much smaller than unity. Thus, for obtaining the requisite expression for  $p/p_\infty$ , we can fruitfully expand in a binomial series:

$$\frac{p}{p_\infty} = \left( \frac{T}{T_\infty} \right)^{\frac{\gamma}{\gamma-1}} \approx \left[ 1 - (\gamma - 1) M_\infty^2 \frac{u}{V_\infty} \right]^{\frac{\gamma}{\gamma-1}} \approx 1 - \gamma M_\infty^2 \frac{u}{V_\infty}.$$

Substituting this in the general expression for pressure coefficient, we finally obtain

$$c_p \approx -2 \frac{u}{V_\infty}. \quad (12)$$

This is the same expression as in the incompressible thin airfoil theory! One must recall that it holds for compressible flow only under the restrictive assumptions delineated in eqn (7).

### 3 Linearized subsonic aerodynamics

In this section, we primarily follow Shapiro [1953], with some similarity in the treatment of Anderson [2011].

We now proceed to specialize eqn (8) to subsonic freestream conditions. In this case, the equation looks very similar to the standard Laplace equation. We will exploit this resemblance to obtain compressible aerodynamic results as simple ‘corrections’ of corresponding incompressible results; the latter may be obtained from limited experiments or numerical calculations.

#### 3.1 Gothert’s compressibility correction rule

Gothert’s compressibility correction rule is the most accurate; however it is difficult to use. We will derive it first (following Shapiro [1953]), and then obtain subsequent simpler, less accurate, rules from it. We will mainly consider two-dimensional flow for notational convenience; extension to 3D is straightforward.

Recall the linearized perturbation potential equation (see eqn (8)), now stated in terms of the perturbation potential  $\phi$ :

$$(1 - M_\infty^2) \frac{\partial^2 \phi}{\partial x^2} + \frac{\partial^2 \phi}{\partial z^2} = 0.$$

This is subjected to the far-field boundary condition

$$\phi \rightarrow 0 \quad \text{as} \quad x, z \rightarrow \pm\infty.$$

The (slip) wall boundary condition states that the airfoil surface must be a streamline of the flow. Denoting coordinates of points on the airfoil surface by  $(x_s, z_s)$ , the wall boundary condition is

$$\frac{dx}{U} = \frac{dz}{W}, \quad \text{on } x_s, z_s.$$

However,  $U = V_\infty + u$  and  $W = w$ ; moreover the thin airfoil assumption (see the first assumption in eqn (7)) is used to conclude that

$$\frac{dz}{dx} = \frac{W}{U} \approx \frac{w}{V_\infty} = \frac{1}{V_\infty} \frac{\partial \phi}{\partial z}, \quad \text{on } x_s, z_s.$$

The governing equation along with the two boundary conditions closely resemble the setup of incompressible thin airfoil theory. To make the connection, consider the change of variables

$$x' = \lambda_x x, \quad z' = \lambda_z z, \quad \phi' = \lambda_\phi \phi, \quad V'_\infty = \lambda_{V_\infty} V_\infty.$$

The new variables will be subsequently shown to be incompressible counterparts of the original variables. Also let  $\beta := \sqrt{1 - M_\infty^2}$ . Then, linearized perturbation potential equation becomes

$$\beta^2 \frac{\lambda_x^2}{\lambda_\phi} \frac{\partial^2 \phi'}{\partial x'^2} + \frac{\lambda_z^2}{\lambda_\phi} \frac{\partial^2 \phi'}{\partial z'^2} = 0.$$

If we set  $\lambda_z/\lambda_x = \beta$ , we recover the incompressible potential flow equation (Laplace equation)  $\nabla'^2 \phi' = 0$ . Here,  $\nabla'$  denotes the gradient operator in the new coordinates.

Transformation of the far-field boundary condition does not reveal anything new:

$$\phi' \rightarrow 0 \quad \text{as } x', z' \rightarrow \pm\infty.$$

Finally, transformation of the wall boundary condition reveals

$$\frac{\lambda_x}{\lambda_z} \frac{dz'}{dx'} = \frac{\lambda_z \lambda_{V_\infty}}{\lambda_\phi} \frac{1}{V'_\infty} \frac{\partial \phi'}{\partial z'}, \quad \text{on } x'_s, z'_s.$$

If we set  $\lambda_\phi/\lambda_{V_\infty} = \lambda_z^2/\lambda_x$ , we recover the incompressible flow wall boundary condition.

**Interim summary:**  $\phi'(x', z')$  describes the incompressible flow past a new airfoil profile  $(x'_s, z'_s)$ , provided that  $\lambda_z/\lambda_x = \beta$  and  $\lambda_\phi/\lambda_{V_\infty} = \lambda_z^2/\lambda_x$ .

### 3.1.1 Relation between geometries of corresponding profiles

Consider the ratio of body slopes in the compressible case and its incompressible counterpart:

$$\frac{dz'_s}{dx'_s} = \frac{\lambda_z}{\lambda_x} \frac{dz_s}{dx_s} = \beta \frac{dz_s}{dx_s}.$$

Thus, all slopes of the airfoil profile (including angle-of-attack  $\alpha$ , camber function (as a fraction of chord)  $z_c$ , and thickness function (as a fraction of chord)  $z_t$ ) in the ‘incompressible’ counterpart must be lesser by the factor  $\sqrt{1 - M_\infty^2}$  than those of the ‘compressible’ case of interest. Formally,

$$\frac{\alpha'}{\alpha} = \frac{z'_c}{z_c} = \frac{z'_t}{z_t} = \beta,$$

where primes denote incompressible counterparts (and not derivatives!).



### 3.1.2 Relation between forces on corresponding profiles

The pressure coefficient  $c_{p,s}$  at a point on the surface of the airfoil in compressible flow can be related to the pressure coefficient  $c'_{p,s}$  at the corresponding point on the surface of its incompressible counterpart as follows (refer to eqn (12)):

$$\frac{c_{p,s}}{c'_{p,s}} \approx \frac{-2u_s/V_\infty}{-2u'_s/V'_\infty} = \lambda_{V_\infty} \frac{(\partial\phi/\partial x)|_{x_s, z_s}}{(\partial\phi'/\partial x')|_{x'_s, z'_s}} = \lambda_{V_\infty} \frac{(\partial\phi/\partial x)|_{x_s, z_s}}{\lambda_\phi/\lambda_x (\partial\phi/\partial x)|_{x_s, z_s}} = \frac{\lambda_{V_\infty} \lambda_x}{\lambda_\phi} = \frac{1}{\beta^2}.$$

Since the sectional lift and moment coefficients are essentially determined by the surface pressure coefficient, they also bear the same ratios; viz.

$$\frac{c_l}{c'_l} = \frac{c_m}{c'_m} = \frac{1}{\beta^2} = \frac{1}{1 - M_\infty^2}.$$

Thus, the ‘incompressible’ counterpart’s sectional lift and moment coefficients should be *scaled up* by  $\beta^{-2}$  to get the corresponding compressible case’s coefficients.

**In summary:** Gothert’s rule states that

$$\text{If } \frac{dz'_s/dx'_s}{dz_s/dx_s} = \frac{\alpha'}{\alpha} = \frac{z'_c}{z_c} = \frac{z'_t}{z_t} = \beta = \sqrt{1 - M_\infty^2}, \quad \text{then } \frac{c_{p,s}}{c'_{p,s}} = \frac{c_l}{c'_l} = \frac{c_m}{c'_m} = \frac{1}{\beta^2}. \quad (13)$$

### 3.1.3 Usage

Gothert’s rule, as derived above, may be used as follows. As an example, to obtain the  $M_\infty = 0.6$  flow over a NACA 5410 airfoil at  $5^\circ$  angle of attack, one needs to refer to the (known) incompressible flow over a NACA 4408 airfoil at  $4^\circ$  angle of attack (since  $\beta = \sqrt{1 - 0.6^2} = 0.8$ ); see figure 2. If the sectional lift coefficient in the incompressible tests (or calculations) is found to be 0.8, say, then the predicted sectional lift coefficient for the original compressible case is 1.25. On the other hand, if the aerodynamic coefficients for the same airfoil is desired at  $M_\infty = 0.5$ , then there is no standard NACA 4-digit airfoil whose incompressible test results we can use directly.

In general, to predict the compressible aerodynamics of a particular airfoil, one has to search for incompressible flow results of a different (scaled down) airfoil. In particular, if one were considering incompressible flow experiments to generate compressible flow data at increasing Mach numbers for a particular airfoil, one has to manufacture a series of airfoils

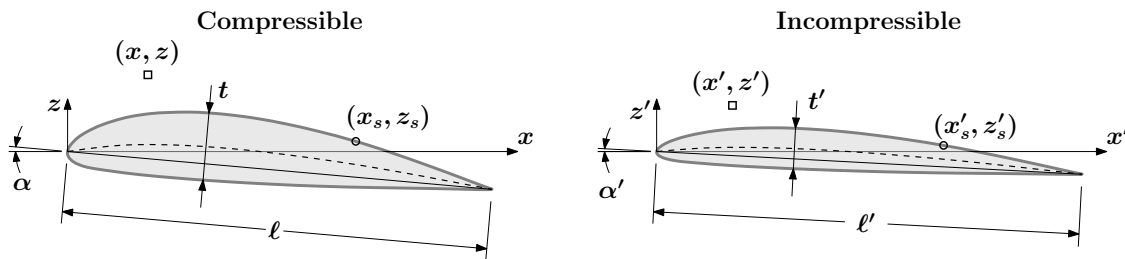


Figure 2: Coordinate transformation for Gothert’s rule [adapted from Shapiro [1953]].

of increasing slenderness (and run tests at decreasing angles of attack). Thus, Gothert's rule is awkward in actual usage.

However, we note that, apart from the assumptions already made in deriving the linearized perturbation potential equations, there are no further constraints on the usage of Gothert's rule.

### 3.2 Prandtl-Glauert Compressibility Correction

The Prandtl-Glauert compressibility correction is much simpler to use compared to Gothert's rule; however, it involves further approximations. The differences are most pronounced in 3D. We will derive this rule starting from Gothert's rule above, following Shapiro [1953]. A different heuristic derivation is given by Anderson [2011].

Consider *incompressible* flow over two similar (affine) airfoil profiles whose thickness, camber and angle of attack are all related by a constant ratio, say  $\delta$ . Then, thin airfoil theory shows that perturbations to the flow, and hence the surface  $c_p$ , will also scale by the same factor  $\delta$ . (Think of the *linear* lift curve, as well as linear dependence of  $\alpha_{L=0}$  on the maximum camber for a family of airfoils.) We denote the variables in the original incompressible case by  $(\cdot)'$  (just as in the setup for Gothert's rule), and those in the scaled case by  $(\cdot)^0$ . (This latter notation is different from that in Shapiro [1953], but agrees with the one used by Anderson [2011].) Thus, formally,

$$\text{If } \frac{dz_s^0/dx_s^0}{dz_s'/dx_s'} = \delta, \quad \text{then } \frac{c_{p,s}^0}{c_{p,s}'} \approx \delta.$$

Combining this with Gothert's rule, and setting  $\delta = \beta^{-1}$  such that

$$\frac{dz_s^0/dx_s^0}{dz_s'/dx_s'} = \frac{dz_s^0/dx_s^0}{dz_s'/dx_s'} \left( \frac{dz_s/dx_s}{dz_s'/dx_s'} \right)^{-1} = \delta (\beta^{-1})^{-1} = 1,$$

(i.e., the same profile!), we have

$$\frac{c_{p,s}}{c_{p,s}^0} = \frac{c_{p,s}}{c_{p,s}'} \frac{c_{p,s}'}{c_{p,s}^0} = \frac{1}{\beta^2} \frac{1}{\delta} = \frac{1}{\beta}.$$

**In summary:** Prandtl-Glauert's rule states that

$$\text{If } \frac{dz_s^0/dx_s^0}{dz_s/dx_s} = \frac{\alpha^0}{\alpha} = \frac{z_c^0}{z_c} = \frac{z_t^0}{z_t} = 1, \quad \text{then } \frac{c_l}{c_l^0} = \frac{c_m}{c_m^0} = \frac{c_{p,s}}{c_{p,s}^0} = \frac{1}{\beta} = \frac{1}{\sqrt{1 - M_\infty^2}}. \quad (14)$$

That is, for the same profile,  $c_p$ ,  $c_l$  and  $c_m$  are all affected by compressibility in proportion to  $(1 - M_\infty^2)^{-1/2}$ . In particular, the lift slope increases as  $(1 - M_\infty^2)^{-1/2}$  with increasing  $M_\infty$ . (The notation for the 'incompressible' case reinforces the fact that  $M_\infty = 0$  for this but the airfoil profile is the same as in the compressible flow case.)

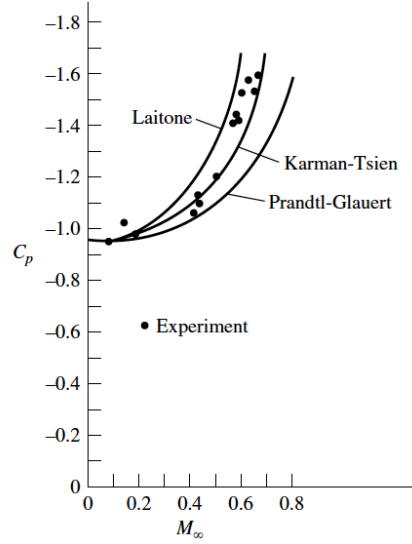


Figure 3: Several compressibility corrections compared with experimental results for the pressure coefficient at the 0.3-chord location of an NACA 4412 airfoil with  $\alpha = 1^\circ 53'$  [Anderson, 2011].

### 3.3 Necessary slenderness of high-speed airfoils

It is profitable to carry on the foregoing analysis one step further, and consider incompressible flow over two affine airfoil profiles such that the  $\delta$  above is  $1/\beta^2$ . We denote the variables in the original incompressible case by  $(\cdot)'$  (just as in the setup for Gothert's rule), and those in the new scaled case by  $(\cdot)'''$  (the notation carrying over from Shapiro [1953]). Then, the preceding developments directly lead to the result

$$\text{If } \frac{dz_s'''/dx_s'''}{dz_s/dx_s} = \frac{\alpha'''}{\alpha} = \frac{z_c'''}{z_c} = \frac{z_t'''}{z_t} = \frac{1}{\sqrt{1 - M_\infty^2}}, \quad \text{then } \frac{c_{p,s}}{c_p'''} = \frac{c_l}{c_l'''} = \frac{c_m}{c_m'''} = 1. \quad (15)$$

That is,  $c_p$ ,  $c_l$  and  $c_m$  will be same for compressible and incompressible flow if the corresponding airfoil profiles are affinely related such that the compressible case's profile is smaller in camber, thickness and angle of attack w.r.t. the incompressible case's profile by the factor  $\sqrt{1 - M_\infty^2}$ .

Boundary layer separation is primarily a function of  $c_p$  distribution. Thus, if an incompressible flow separates from an airfoil profile of a certain thickness, camber and angle of attack, then a high-speed (compressible) flow will separate from an even thinner profile with smaller camber and at a lower angle of attack. Thus, *high-speed airfoils must be thinner and less cambered than low-speed ones, and operate at lower angles of attack.*

### 3.4 Improved (nonlinear) compressibility corrections

The neglect of nonlinearity in the foregoing analysis sometimes leads to appreciable errors in some cases. Improved predictions are obtained by accounting for some aspects of the nonlinearity. As discussed by Anderson [2011], Karman-Tsien rule gives the pressure coefficient

at a point in compressible flow  $c_p$  as

$$c_p = \frac{c_p^0}{\sqrt{1 - M_\infty^2} + [M_\infty^2/(1 + \sqrt{1 - M_\infty^2})]c_p^0/2}, \quad (16)$$

where  $c_p^0$  is the pressure coefficient at the same point in incompressible flow (continuing with the notation introduced for the Prandtl-Glauert correction). The reader should *NOT* try to memorize this expression; instead it should only be noted that  $c_p$  is no longer a linear function of  $c_p^0$ . The more recent Laitone correction is also similar in form; both give better predictions than the Prandtl-Glauert method (see figure 3).

## 4 Estimation of critical Mach number

It will be recalled that the critical Mach number,  $M_{cr}$  is the freestream Mach number at which the maximum Mach number is unity (sonic) in the flow over a given airfoil at a particular angle of attack. Estimation of this is desired (e.g. so as to stay away from transonic effects).

Let us term the pressure coefficient at the point where the flow reaches sonic condition for  $M_\infty = M_{cr}$  as the critical pressure coefficient,  $c_{p,cr}$ . Then, we can find two alternative relations between  $c_{p,cr}$  to  $M_{cr}$  – one from thermodynamics and another from aerodynamics. These equations, when solved simultaneously, yield the desired  $M_{cr}$ .

**Thermodynamic relation between  $c_{p,cr}$  and  $M_{cr}$ :** Consider a point  $A$  in a flow. We wish to relate the pressure coefficient at  $A$ ,  $c_{p,A}$ , to the local Mach number,  $M_A$  and the freestream Mach number  $M_\infty$ . This is possible in case of isentropic flow throughout the domain, in which case we have (invoking the general expression for  $c_p$  in eqn (11) without additional assumptions)

$$c_{p,A} = \frac{2}{\gamma M_\infty^2} \left( \frac{p_A}{p_\infty} - 1 \right) = \frac{2}{\gamma M_\infty^2} \left( \frac{p_A}{p_0} \frac{p_0}{p_\infty} - 1 \right) = \frac{2}{\gamma M_\infty^2} \left[ \left\{ \frac{1 + (\gamma - 1)M_\infty^2/2}{1 + (\gamma - 1)M_A^2/2} \right\}^{\frac{\gamma}{\gamma-1}} - 1 \right].$$

Specializing to the critical condition wherein  $M_\infty = M_{cr}$ ,  $M_A = 1$  and  $c_{p,A} = c_{p,cr}$ , we have

$$c_{p,cr} = \frac{2}{\gamma M_{cr}^2} \left[ \left\{ \frac{1 + (\gamma - 1)M_{cr}^2/2}{1 + (\gamma - 1)/2} \right\}^{\frac{\gamma}{\gamma-1}} - 1 \right].$$

(Note that the isentropic flow assumption is valid since the critical condition is free of shocks.) This expression is not specific to any particular airfoil. Instead, it simply expresses a thermodynamic relation between the pressure and Mach number in an isentropic flow; it is depicted as curve  $C$  in figure 4a. Being a relation between  $c_{p,cr}$  and  $M_{cr}$ , it is not useful in determining either of these quantities by itself in isolation.

**Aerodynamic relation between  $c_{p,cr}$  and  $M_{cr}$ :** An alternate relation between the critical pressure coefficient and the critical Mach number can be obtained from aerodynamics.

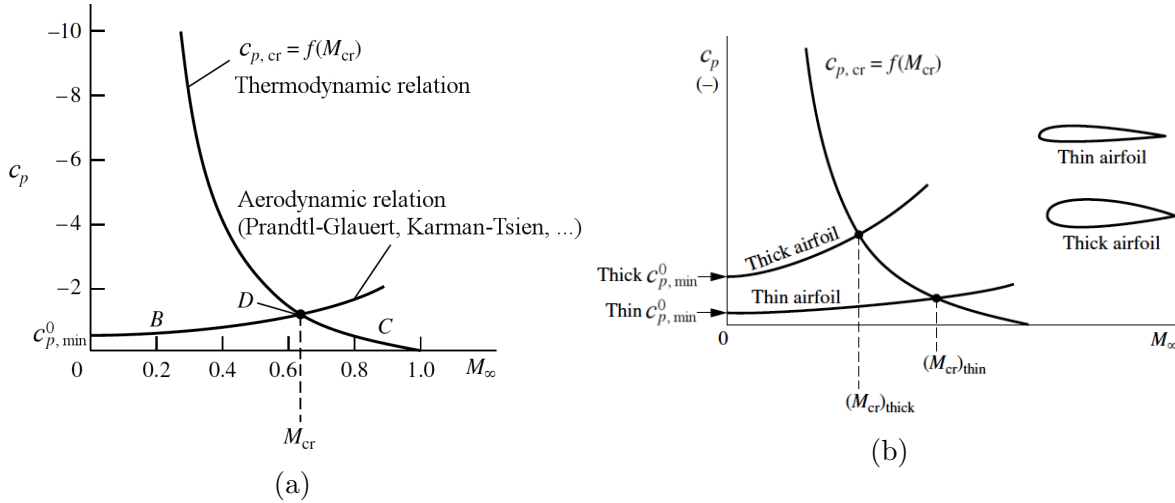


Figure 4: (a) Estimation of critical Mach number. (b) Effect of airfoil thickness on critical Mach number. (Adapted from Anderson [2011].)

First, we show that the point of minimum pressure on an airfoil does not change with compressibility. To start with, per the linear Prandtl-Glauert theory (see eqn (14)), the  $c_p$  at all points scale together as  $1/\sqrt{1 - M_\infty^2}$ , so that the point of minimum pressure remains as such for all  $M_\infty$  values. Even in case of the nonlinear Karman-Tsien theory, we note from eqn (16) that

$$\frac{\partial c_p}{\partial c_p^0} = \frac{\sqrt{1 - M_\infty^2}}{\left[ \sqrt{1 - M_\infty^2} + \left\{ M_\infty^2 / (1 + \sqrt{1 - M_\infty^2}) \right\} c_p^0 / 2 \right]^2}.$$

This indicates that if a point on the airfoil has the least pressure in incompressible flow (most negative  $c_p^0$ ), then it will also have the largest  $\partial c_p / \partial c_p^0$  at all values of  $M_\infty$ , thereby continuing to encounter the minimum pressure in all compressible flow cases. The same conclusion is reached from Laitone's theory.

The above observation points to an aerodynamic relation between  $c_{p,cr}$  and  $M_{cr}$ . In particular, let  $c_{p,min}^0$  denote the minimum pressure coefficient in incompressible flow over the airfoil of interest at the desired angle of attack. Then, curve B in figure 4a depicts the pressure coefficient at this point with increasing  $M_\infty$  using a suitable compressibility correction (be it Prandtl-Glauert, Karman-Tsien, Laitone, or any other). But, since this is the minimum  $c_p$  on the airfoil, it will attain the critical value  $c_{p,cr}$  when  $M_\infty$  becomes  $M_{cr}$ .

In summary, the intersection of the thermodynamic and aerodynamic relations yields the desired estimate of the critical Mach number.

**Effect of airfoil thickness on  $M_{cr}$ :** The foregoing graphical method for estimating  $M_{cr}$  has another advantage – it forcefully demonstrates the crucial effect of airfoil thickness on  $M_{cr}$ . Referring to figure 4b, we realize that, all other aspects being equal, the magnitude of the minimum pressure coefficient achieved in *incompressible* flow over an airfoil is a monotonically increasing function of the airfoil thickness. This can also be understood from thin airfoil theory – the thinner the airfoil, the less perturbation it causes to the background flow,

and the lower is the departure of the surface pressure from the freestream condition. Then, linear (Prandtl-Glauert) compressibility correction, as well as nonlinear theory, show that the corresponding aerodynamic relation curves are as depicted in figure 4b.

One concludes that *the critical Mach number is higher on a thinner airfoil*. The benefit of a thinner airfoil in reducing flow separation at high  $M_\infty$  has already been discussed. Thus, slenderness of the airfoil is of crucial importance in the design of transonic and supersonic aircraft.

## 5 Supersonic aerodynamics in two dimensions

Upending expectations, aerodynamics tends to get simpler as the freestream becomes supersonic. Shocks and expansion fans are indeed encountered, but these are well-modelled local phenomena. Neglecting viscous effects, however, may lead to inaccuracies in predictions. This is especially true where shock waves interact with the boundary layer leading to intense unsteadiness. In the preliminary analysis pursued here, we will continue to neglect viscous effects.

There are two main simplified theories for two-dimensional supersonic aerodynamics

1. Linear theory for airfoils with slender and smooth profiles at small  $\alpha$ , and
2. Shock-expansion theory for airfoils of arbitrary thickness at arbitrary  $\alpha$ , as long as the airfoils are made of straight sections, or can be approximated as such.

Both these theories require the leading edge to be very sharp. This is not a restriction since supersonic airfoils are indeed designed with very sharp leading edges to avoid strong bow shocks that increase drag. In the subsequent analysis, it will be evident that fundamental differences exist between subsonic and supersonic aerodynamics, which has to do with the fundamentally different mathematical character of subsonic and supersonic flows.

### 5.1 Linearized supersonic aerodynamics in 2D

In this section, we follow Anderson [2011].

We have already derived the linearized perturbation potential equation

$$(M_\infty^2 - 1) \frac{\partial^2 \phi}{\partial x^2} - \frac{\partial^2 \phi}{\partial z^2} = 0, \quad (17)$$

which is valid if the airfoil is thin and gently cambered, and it encounters moderately supersonic flow (i.e.  $M_\infty$  between about 1.2 and 5) at low angles of attack. The thin-airfoil assumption is even more justified in supersonic aerodynamics as airfoil sections designed for supersonic flight are generally very thin indeed (reasons for which have been discussed previously).

Note that the above linearized theory is *not* valid for flows with shocks, which are essentially non-isentropic and nonlinear phenomena. However, it turns out that if the airfoil is very slender and is at a very small angle of attack, then the shocks are very weak too. We will direct our attention to this scenario.

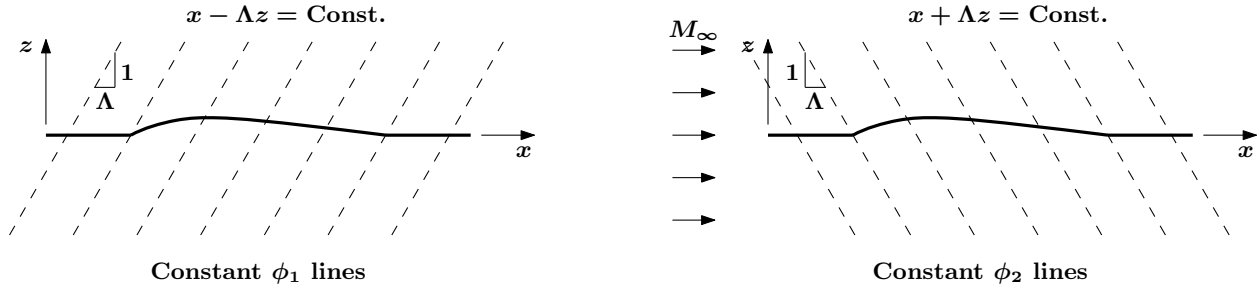


Figure 5: Characteristics in linearized supersonic aerodynamics.

Defining  $\Lambda := \sqrt{M_\infty^2 - 1} > 0$  for supersonic freestream, the governing equation for *perturbations* can be rewritten as

$$\Lambda^2 \frac{\partial^2 \phi}{\partial x^2} - \frac{\partial^2 \phi}{\partial z^2} = 0. \quad (18)$$

This further clarifies the fact that we have a *hyperbolic* linear PDE, meaning that

- perturbations propagate as waves,
- perturbations (or ‘information’) does not propagate upstream (into the supersonic flow), and
- boundary conditions need to be specified at the ‘inflow’ and ‘wall’ only.

Under the prevailing assumptions of linearized supersonic flow over slender bodies at low  $\alpha$ , a radical phenomenon is observed –  $x$  and  $z$ –coordinates become linked in the solution. That is, the general solution can be verified to be

$$\phi(x, z) = \phi_1(x - \Lambda z) + \phi_2(x + \Lambda z). \quad (19)$$

This shows that the solution is a linear combination of two (as yet undetermined) functions, each of one variable only.

Lines of constant  $\phi_1$  (called characteristics) are parallel lines with  $x - \Lambda z = \text{Const.}$ , and those of constant  $\phi_2$  are also parallel lines but with  $x + \Lambda z = \text{Const.}$  (see figure 5). It is readily verified that the characteristics are Mach lines for the flow, i.e., they make the familiar Mach angle (viz.  $\sin^{-1}(1/M_\infty)$ ) with the freestream direction.

Suppose a slender surface is immersed in this supersonic flow. The presence of the bump cannot be ‘felt’ upstream in the supersonic flow. If the solution for  $\phi$  has non-trivial  $\phi_2$ , then it would mean ‘communicating’ the presence of the bump upstream. In particular,  $\phi_2$  must change at the bump leading edge due to the bump, but this change will appear upstream! Thus, only  $\phi_1$  can be non-trivial ‘above’ the surface (i.e., in increasing  $z$ -direction). By the same argument, only  $\phi_2$  can be non-trivial below the surface (i.e., in decreasing  $z$ -direction). Notice how simple the solution is already.

Summarizing the preceding arguments, figure 6 depicts the geometry of linearized aerodynamics solution for supersonic flow over an immersed body. Specifically, the perturbation potential solution consists of  $\phi_1(x - \Lambda z)$  ‘above’ the body, and  $\phi_2(x + \Lambda z)$  ‘below’ the body, when flow is from left to right. Upstream and downstream of the body, both functions are trivially uniform (and hence, not depicted).

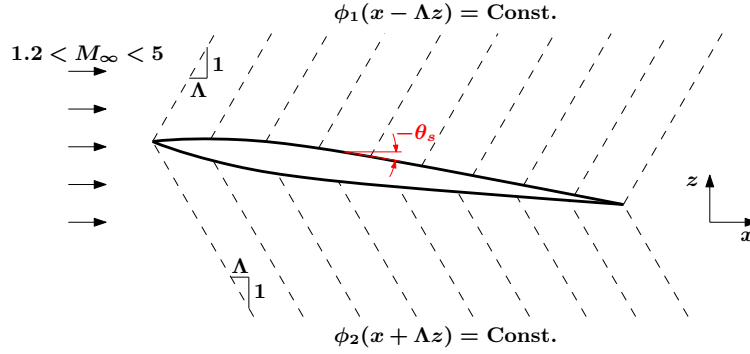


Figure 6: Solution of linearized supersonic aerodynamics over an immersed body.

**Question:** How do you explain that streamlines should be perpendicular to equipotential lines, and the flow should be primarily in the  $x$ -direction?

Now, all that remains to be determined are the actual functions  $\phi_1$  and  $\phi_2$ ; these are anticipated to depend on the wall boundary condition. We start by noting that above the body, the perturbation velocity components are

$$u = \frac{\partial \phi}{\partial x} = \frac{\partial \phi_1}{\partial x} = \phi'_1, \quad w = \frac{\partial \phi}{\partial z} = \frac{\partial \phi_1}{\partial z} = -\Lambda \phi'_1, \quad \text{above the body.}$$

where  $\phi'_1$  denotes the derivative of  $\phi_1$  with respect to its sole argument. Similarly, below the body, we have

$$u = \frac{\partial \phi}{\partial x} = \frac{\partial \phi_2}{\partial x} = \phi'_2, \quad w = \frac{\partial \phi}{\partial z} = \frac{\partial \phi_2}{\partial z} = \Lambda \phi'_2, \quad \text{below the body.}$$

But, this indicates a particularly simple relation between the two components of velocity perturbation at any point in the flow, viz.

$$u = -\frac{w}{\Lambda} \quad \text{above the body,} \quad \text{and} \quad u = \frac{w}{\Lambda} \quad \text{below the body.}$$

Recalling that the (slender) body must be a streamline of the flow, the slope of the surface at any point is  $dz_s/dx_s = \tan \theta_s \approx \theta_s$ , where  $\theta_s$  is the angle that the local surface makes with the freestream, and it is assumed to be small under the restrictions of linear theory (see figure 6). But, for the surface to be a streamline of the flow, we have the following relation (note that the *full* velocity must be used, and not the perturbation quantity)

$$\frac{dx_s}{U_s} = \frac{dz_s}{W_s} \quad \implies \quad \theta_s \approx \frac{dz_s}{dx_s} = \frac{W_s}{U_s} = \frac{w_s}{V_\infty + u_s} \approx \frac{w_s}{V_\infty}.$$

Thus, the local  $z$ -component of perturbation velocity is related to the local slope of the body surface. Using the preceding relations found between the two components of perturbation velocity, we have

$$u_s = \begin{cases} -V_\infty \theta_s / \Lambda & \text{on the upper surface,} \\ V_\infty \theta_s / \Lambda & \text{on the lower surface.} \end{cases}$$



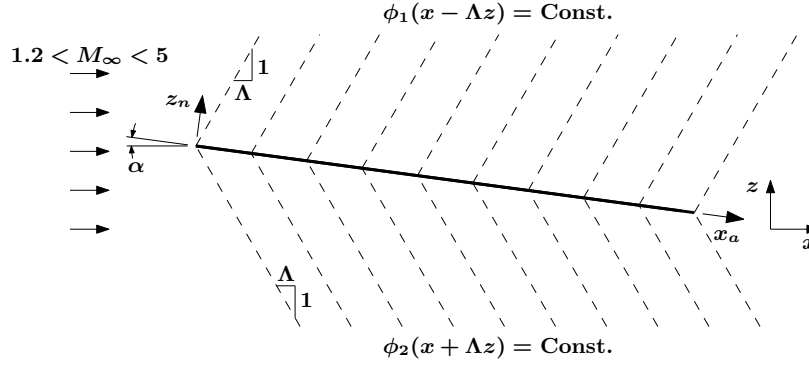


Figure 7: Solution of linearized supersonic aerodynamics over an immersed flat plate.

The above expression can now be used in the simplified expression for pressure coefficient derived for linearized aerodynamics in eqn (12), viz.  $c_p \approx -2u/V_\infty$ . Thus, we have

$$c_{p,s} = \begin{cases} \frac{2\theta_s}{\sqrt{M_\infty^2 - 1}} & \text{on the upper surface,} \\ -\frac{2\theta_s}{\sqrt{M_\infty^2 - 1}} & \text{on the lower surface.} \end{cases} \quad (20)$$

Thus, there is a very simple geometric expression for the pressure coefficient on a slender airfoil in supersonic flow, under the assumptions of linear theory. Note from figure 6 that  $\theta_s$  is typically negative on the suction surface (upper surface for positive  $\alpha$ ) so that  $c_{p,s} < 0$  thereat. Analogously,  $\theta_s$  is typically negative again on the pressure surface (lower surface for positive  $\alpha$ ) so that  $c_{p,s} > 0$  thereat. Thus, the major portions of both surfaces contribute positively to the lift, as anticipated.

### 5.1.1 Flat plate at small $\alpha$

Consider a flat plate immersed in a supersonic flow (freestream Mach number  $M_\infty$ ) at a small angle of attack  $\alpha$ . The angle of the body surface relative to the freestream is  $\theta_s = -\alpha$  everywhere. Thus, linear theory gives  $c_{p,u} = -2\alpha/\sqrt{M_\infty^2 - 1}$  and  $c_{p,l} = 2\alpha/\sqrt{M_\infty^2 - 1}$ . That is, the pressure coefficient is constant throughout the length of the plate (very unlike the corresponding subsonic case!), and it is equal in magnitude and opposite in sign on the upper and lower surfaces.

To determine  $c_l$ , we first compute the normal and axial force coefficients (refer to figure 7),

$$c_n = \frac{1}{c} \int_{LE}^{TE} (c_{p,l} - c_{p,u}) dx_a = \frac{4\alpha}{\sqrt{M_\infty^2 - 1}}, \quad c_a = \frac{1}{c} \int_{LE}^{TE} (c_{p,l} - c_{p,u}) dz_n = 0.$$

Using these, we find the lift (and drag!) coefficients

$$c_l = c_n \cos \alpha - c_a \sin \alpha \approx \frac{4\alpha}{\sqrt{M_\infty^2 - 1}}, \quad c_d = c_n \sin \alpha + c_a \cos \alpha \approx \frac{4\alpha^2}{\sqrt{M_\infty^2 - 1}}. \quad (21)$$

We thus find that, even in the absence of shocks (and viscous effects), inviscid supersonic flow results in drag (called wave drag).

**Question:** What is the origin of the wave drag in the above problem? Why does D'Alembert's paradox not extend to supersonic aerodynamics?

It will be recalled that the center of pressure was at the quarter-chord point for a flat plate in incompressible flow. Let us compute the center of pressure for the present case of a flat plate in supersonic flow. We can do this in two alternative methods: (i) intuitive, and (ii) mathematical.

In the intuitive approach, we recognize that the pressure is uniform throughout the suction surface, as well as throughout the pressure surface. Thus, the resultant pressure forces must act through the center of the plate on both sides; both will be directed 'upward' so as to contribute to positive lift in the case of positive  $\alpha$  depicted in figure 7. Thus, the net lift force must also act through the center of the plate, so that the center of pressure must be the half-chord point; i.e.,

$$x_{cp} = \frac{c}{2}, \quad \text{in (linearized) supersonic flow over flat plate.}$$

This is a drastic change from the low-speed flow result!

In the mathematical approach, we can calculate the pitching moment about a convenient point, say the leading edge. Then, we will look for the point about which the pitching moment vanishes, and of course arrive at the same answer as above.

Next, we realize that the center of pressure found above does not depend on the angle of attack. Thus, we conclude that

$$x_{ac} = \frac{c}{2} \quad \text{and} \quad c_{m,ac} = c_{m,c/2} = 0, \quad \text{in (linearized) supersonic flow over flat plate.}$$

Since most supersonic airfoils are very thin and lightly cambered (if at all), the above result holds true not only for the flat plate but for most supersonic airfoils; see example later.

Finally, consider an aircraft that is to fly supersonic. At take-off, it of course flies at a low subsonic speed, whence the center of pressure is close to the quarter chord point (assuming that the wing is unswept and of high aspect ratio – not a good assumption!). However, when it goes supersonic, the center of pressure moves aft. This must lead to a moment imbalance, which needs to be counteracted very quickly by appropriate control surface movement. Or, better, by some other changes – like redistribution of fuel, as in the Concorde.

## 5.2 Shock-expansion theory of supersonic aerodynamics in 2D

In this section, we follow Anderson [2011].

If instead of making the assumptions of linear supersonic theory, we only assume that

- the airfoil's leading edge is sharp such that there is no bow shock formed thereat, and
- the airfoil geometry is made of straight sections (panels),

then we can numerically solve the problem using knowledge of oblique shocks and expansion fans.

Reconsider the flat plate immersed in the supersonic flow again. As shown in figure 8, the pressure surface will turn the flow into itself, resulting in the oblique shock  $S_{LE}$  attached

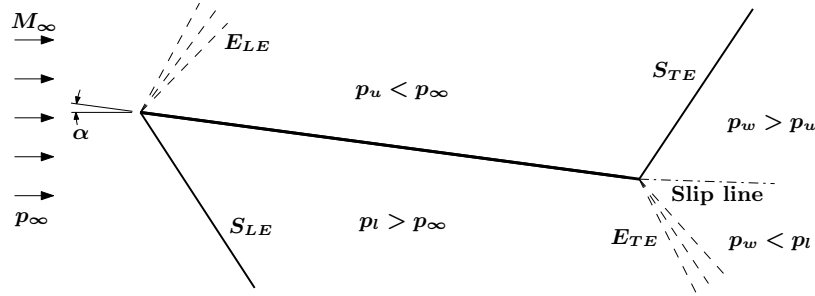


Figure 8: Shock-expansion theory for supersonic flow over an immersed flat plate.

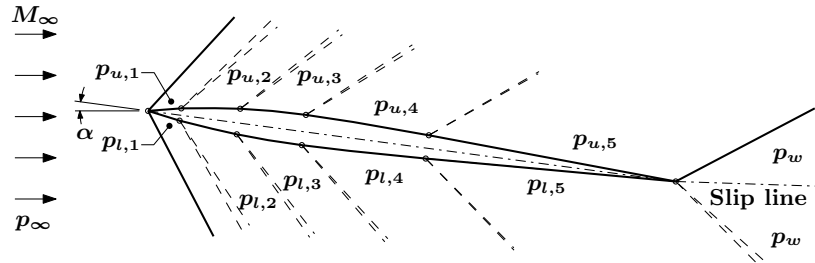


Figure 9: Shock-expansion theory for supersonic flow over a slender body.

at the leading edge. The pressure immediately behind the shock  $p_l$  is necessarily greater than the freestream pressure  $p_\infty$ . Conversely, the suction surface will cause an expansion fan  $E_{LE}$  to form at the leading edge. The pressure behind the expansion fan  $p_u$  is necessarily lesser than  $p_\infty$ . Since there are no changes in the flow direction over the remainder of the flat plate, the pressures on the entire pressure and suction surfaces remain  $p_l$  ( $> p_\infty$ ) and  $p_u$  ( $< p_\infty$ ), respectively. This pressure difference accounts for the lift on the flat plate.

By the same token, there will be opposite flow systems at the trailing edge, viz. an expansion fan  $E_{TE}$  at the pressure surface and an oblique shock  $S_{TE}$  at the suction surface. In the prevailing theory, the aerodynamic predictions are independent of the flow in the wake. However, we note that a slip line will be formed in the wake such that the pressure  $p_w$  is same on both sides. In fact, the angle of the slip line itself is determined by simultaneously solving for the same pressure behind  $E_{TE}$  and  $S_{TE}$ .

The lift, wave drag and moment coefficients depend only on  $p_l$  and  $p_u$ . Analytical expressions for these are complicated. However, these can be solved for exactly from the theories of oblique shocks and expansion fans using appropriate look-up tables.

### 5.2.1 Example of an airfoil

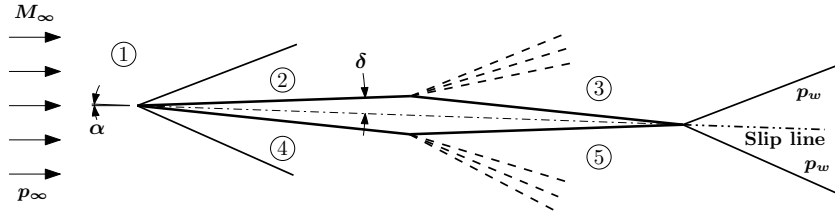
Now, consider the supersonic flow over a generic bi-convex airfoil (as appropriate for supersonic aircraft) at an angle of attack  $\alpha$  (see figure 9). Just as in incompressible panel method, we can discretize the surface of the airfoil into a set of flat panels. Then, the shock expansion theory predicts oblique shocks or expansion fans at junction between each pair of adjacent panels, as depicted in figure 9.

For positive  $\alpha$ , there will typically be a leading edge shock on the pressure surface. Whether there is a shock or an expansion fan at the leading edge on the suction surface de-

depends on its half-wedge angle (w.r.t. the chord line) and on the  $\alpha$ . At successive downstream panel junctions of the pressure surface, typically there will be expansion fans since the surface is usually convex (i.e., slope increases monotonically). Similarly, typically there will be a series of expansion fans at successive downstream panel junctions on the suction surface too, as it is also convex usually (i.e., its slope decreases monotonically). Note that, even if the airfoil is symmetric, the expansion fans at corresponding junctions of the upper and lower surface will not be identical in strength since their respective upstream Mach numbers will usually be different. In any case, one can determine the pressure on the various panels from shock-expansion theory, and finally calculate the requisite lift and moment coefficients therefrom.

For slender airfoils at small  $\alpha$ , the shocks and expansion fans would all be very weak (due to small rotations experienced by the flow at the junctions). Thus, the departure of the local Mach number from the freestream value may not be significant. But this is precisely the assumption of the preceding linear theory. Thus, numerical results are expected to be similar from the two theories.

**Question (Shock-expansion solution for double-wedge airfoil flow):** Find the lift, wave drag and pitching moment coefficients of a double-wedge airfoil with half-wedge angle of  $\delta = 4^\circ$  placed in a  $M_\infty = 3$  flow at  $\alpha = 2^\circ$ .



**Solution:** Consider the leading edge on the upper surface, where the supersonic flow is turned into itself by  $\theta_1 = \delta - \alpha = 2^\circ$ . Referring to the oblique-shock graph, the upstream  $M_1 = 3$  and  $\theta_1 = 2^\circ$  yield shock angle  $\beta_1 = 21^\circ$ . This means that the upstream Mach number normal to the shock is  $M_{n,1} = M_\infty \sin \beta_1 = 1.07$  (notice how close this is to sonic condition). Referring to the normal shock tables, the corresponding downstream normal Mach number is  $M_{n,2} = 0.94$ . Then, the Mach number of the flow behind the oblique shock is  $M_2 = M_{n,2} / \sin(\beta_1 - \theta_1) = 2.9$  (notice how small the decrease is from  $M_\infty$ ). Also, the static pressure ratio is  $p_2/p_\infty = p_2/p_1 = 1.17$  (notice how slight the *increase* is from  $p_\infty$ ).

The flow conditions remain constant over the fore section of the upper surface, until it encounters the expansion corner at the mid-chord. Here, the turning angle for the flow is  $\theta_2 = 2\delta = 8^\circ$ . Referring to the expansion fan tables, the Prandtl-Meyer function for  $M_2 = 2.9$  is  $\nu_2 = 47.8^\circ$ . Adding the turning angle, the P-M function downstream of the expansion fan should be  $\nu_3 = \nu_2 + \theta_2 = 55.8^\circ$ . This yields the downstream Mach number as  $M_3 = 3.3$ . Also, the static pressure ratio (using the isentropic nature of the

expansion fan to conclude that  $p_{0,3} = p_{0,2}$ ) is

$$\frac{p_3}{p_2} = \frac{p_{0,2}/p_2}{p_{0,3}/p_3} = \left[ \frac{1 + 0.5(\gamma - 1)M_2^2}{1 + 0.5(\gamma - 1)M_3^2} \right]^{\frac{\gamma}{\gamma-1}} = 0.53.$$

Thus,  $p_3/p_\infty = (p_2/p_\infty) \times (p_3/p_2) = 0.61$ . (This is a significant pressure suction.) This pressure prevails over the aft section of the upper surface.

Now consider the leading edge again, but on the lower surface, where the turning angle is  $\theta'_1 = \delta + \alpha = 6^\circ$ . Referring to the oblique-shock graph, the upstream  $M_1 = 3$  and  $\theta'_1 = 6^\circ$  yield shock angle  $\beta'_1 = 24^\circ$ . This means that the upstream Mach number normal to the shock is  $M'_{n,1} = M_\infty \sin \beta'_1 = 1.22$ . Referring to the normal shock tables, the corresponding downstream normal Mach number is  $M_{n,4} = 0.83$ . Then, the Mach number of the flow behind the oblique shock is  $M_4 = M_{n,4} / \sin(\beta'_1 - \theta'_1) = 2.7$ . Also, the static pressure ratio is  $p_4/p_\infty = p_4/p'_1 = 1.56$  (notice how large the *increase* is from  $p_\infty$ ).

The flow conditions remain constant over the fore section of the lower surface, until it encounters the expansion corner at the mid-chord. Here, the turning angle for the flow is  $\theta_4 = 2\delta = 8^\circ$  (same as on the upper surface). However, since  $M_4$  is different from  $M_2$ , the expansion fan properties have to be calculated afresh. Referring to the expansion fan tables, the Prandtl-Meyer function for  $M_4 = 2.7$  is  $\nu_4 = 43.6^\circ$ . Adding the turning angle, the P-M function downstream of the expansion fan should be  $\nu_5 = \nu_4 + \theta_4 = 51.6^\circ$ . This yields the downstream Mach number as  $M_5 = 3.1$ . Also, the static pressure ratio is

$$\frac{p_5}{p_4} = \frac{p_{0,4}/p_4}{p_{0,5}/p_5} = \left[ \frac{1 + 0.5(\gamma - 1)M_4^2}{1 + 0.5(\gamma - 1)M_5^2} \right]^{\frac{\gamma}{\gamma-1}} = 0.55.$$

Thus,  $p_5/p_\infty = (p_4/p_\infty) \times (p_5/p_4) = 0.85$ . (This is a suction!) This pressure prevails over the aft section of the lower surface.

Before we start computing the various coefficients, recall that the dynamic head is  $0.5\rho_\infty V_\infty^2 = 0.5\gamma p_\infty M_\infty^2$ . Exploiting the symmetry of the airfoil, the sectional normal force coefficient can be directly determined as

$$c_n = \frac{(p_4 + p_5 - p_2 - p_3)(\cos \delta)(c/2 \cos \delta)}{0.5\gamma p_\infty M_\infty^2 c} = 0.05.$$

Similarly, the sectional axial force coefficient is

$$c_a = \frac{(p_2 + p_4 - p_3 - p_5)(\sin \delta)(c/2 \cos \delta)}{0.5\gamma p_\infty M_\infty^2 c} = 0.007.$$

This yields the sectional lift coefficient as

$$c_l = c_n \cos \alpha - c_a \sin \alpha = 0.05.$$

Also, the sectional wave drag coefficient is

$$c_{d,wave} = c_n \sin \alpha + c_a \cos \alpha = 0.009.$$

Finally, since the facets of the airfoil are straight and equal, and pressure is uniform over each facet, the pitching moment about the mid-chord (approximating  $\cos \delta \approx 1$ ) is

$$c_{m,c/2} = \frac{(p_3 - p_2 + p_4 - p_5)(0.5c)(0.25c)}{0.5\gamma p_\infty M_\infty^2 c^2} = 0.003.$$

Now, we can find the location of the center of pressure using the moment balance:

$$c_{m,c/2} = -\frac{x_{cp} - c/2}{c} c_l,$$

which gives  $x_{cp}/c = 0.5 - c_{m,c/2}/c_l = 0.44$ . This is definitely not at the half-chord point, but it is much nearer to it than to the quarter-chord point.

**Solution using linear theory:** Let us calculate the above coefficients again, but using linear theory. We refer to eqn (20) for the expressions for  $c_p$  on the upper and lower surfaces. On the fore section of the upper surface,  $\theta_s = +2^\circ$  so that  $c_{p,2} = 0.025$ . On the aft section of the upper surface,  $\theta_s = -6^\circ$  so that  $c_{p,3} = -0.074$ . On the fore section of the lower surface,  $\theta_s = -6^\circ$ , so that  $c_{p,4} = 0.074$ . Finally, on the aft section of the lower surface,  $\theta_s = +2^\circ$ , so that  $c_{p,5} = -0.025$ . (Note that these values do *not* compare too favourably with the coefficients that may be calculated from the values of  $p_2/p_\infty$ , etc. found in the shock-expansion theory, viz.  $c_{p,2} = (p_2/p_\infty - 1)/(0.5\gamma M_\infty^2) = 0.026$ ,  $c_{p,3} = -0.061$ ,  $c_{p,4} = 0.089$  and  $c_{p,5} = -0.023$ .)

Using the geometry of the airfoil, the sectional normal force coefficient is

$$c_n = \frac{(c_{p,4} + c_{p,5} - c_{p,2} - c_{p,3})(\cos \delta)(c/2 \cos \delta)}{c} = 0.049.$$

Similarly,

$$c_a = \frac{(c_{p,2} + c_{p,4} - c_{p,3} - c_{p,5})(\sin \delta)(c/2 \cos \delta)}{c} = 0.007.$$

These are almost identical to the results found earlier. Thus, the lift and wave drag coefficients also turn out to be similar, i.e.  $c_l = 0.049$  and  $c_{d,wave} = 0.009$ . Notice how dissimilarities in  $c_p$  values from the two theories are ameliorated in the final integrated coefficients.

It is easy to see from the symmetry of the problem that the pitching moment vanishes about the half-chord point. So, linear theory predicts that the half-chord point is the center of pressure. This is the same as in the flat plate problem investigated earlier, and also marks a discrepancy from the result found above with the shock-expansion theory.

## Appendix

### A Potentials in linearized supersonic aerodynamics

In the theory of linearized supersonic aerodynamics, the calculation of pressure coefficient and lift/moment coefficients of an airfoil could be pursued without ever actually having to determine the two perturbation potential functions  $\phi_1$  and  $\phi_2$ ; mere knowledge of their forms was sufficient. However, for completeness, here we determine these functions from the wall boundary condition, following Shapiro [1953].

It will be recalled that the general solution for the linearized perturbation potential equation is  $\phi(x, z) = \phi_1(x - \Lambda z) + \phi_2(x + \Lambda z)$ . Then,

$$u = \partial\phi/\partial x = \phi'_1 + \phi'_2, \quad w = \partial\phi/\partial z = \Lambda(\phi'_2 - \phi'_1).$$

In general, the equation of a streamline (with the streamline variables denoted by the subscript *str*) is

$$\left(\frac{dz}{dx}\right)_{str} = \frac{W}{U} = \frac{w}{V_\infty + u} = \frac{w/V_\infty}{1 + u/V_\infty} \approx \frac{w/V_\infty}{1 + u/V_\infty - M_\infty^2 u/V_\infty} = \frac{\Lambda(\phi'_2 - \phi'_1)}{V_\infty - \Lambda^2(\phi'_2 + \phi'_1)},$$

where (to facilitate subsequent integration) we have inserted the extra term  $M_\infty^2 u/V_\infty$  in the fourth step, appealing to its assumed smallness in the prevailing linear theory (see eqn (7)). Rearranging, and temporarily omitting the *str* subscript for notational convenience, we have

$$V_\infty dz = \Lambda(\phi'_2 - \phi'_1)dx + \Lambda^2(\phi'_2 + \phi'_1)dz = \Lambda[(\phi'_2 dx + \Lambda\phi'_2 dz) - (\phi'_1 dx - \Lambda\phi'_1 dz)] = \Lambda[d\phi_2 - d\phi_1],$$

where, the last step is obtained by noting that

$$d\phi_1 = \frac{\partial\phi_1}{\partial x}dx + \frac{\partial\phi_1}{\partial z}dz = \phi'_1 dx - \Lambda\phi'_1 dz,$$

and similarly for  $\phi_2$ .

Integrating, we get the (implicit) equation for a streamline as

$$z_{str} = \Lambda[\phi_2(x_{str} + \Lambda z_{str}) - \phi_1(x_{str} - \Lambda z_{str})]/V_\infty + \text{Const.} \quad (22)$$

One obtains different streamlines by choosing different values of the constant.

Next, we wish to use the above expression to actually determine  $\phi_1$  and  $\phi_2$  based on two known streamlines, viz. the upper and lower surfaces of the slender body. For concreteness, we set the origin of the coordinate system to the leading edge of the slender body. Then, recalling that  $\phi_2$  is trivial above the body and  $\phi_1$  is trivial below it, we have

$$\phi_1(x_u - \Lambda z_u) = -z_u V_\infty / \Lambda, \quad \phi_2(x_l + \Lambda z_l) = z_l V_\infty / \Lambda, \quad \forall x_u, x_l \in [0, c], \quad (23)$$

In the above,  $z_u(x)$  and  $z_l(x)$  are the known functions for the upper and lower surface. We have chosen the constant in the streamline expression to be zero in both cases. Due to the particular choice of the origin of the coordinate system, we thereby obtain that  $\phi_1$  and  $\phi_2$  are both zero on their respective leading edge characteristics.

To use the above equations, consider the problem of determining  $\phi_1$  at a particular point  $(x, z)$  above the airfoil. We have to first trace along the characteristic passing through this point until we reach the upper surface. That is, we have to solve for  $x_u$  from the implicit equation  $x_u - \Lambda z_u(x_u) = x - \Lambda z$ . Then the value of  $\phi_1(x, z)$  is  $-z_u(x_u)V_\infty/\Lambda$ .

## References

- J. D. Anderson. *Fundamentals of aerodynamics*. McGraw-Hill, fifth edition, 2011.
- E. L. Houghton, P. W. Carpenter, S. H. Colicott, and D. T. Valentine. *Aerodynamics for engineering students*. Elsevier, 7th edition, 2013.
- A. H. Shapiro. *The dynamics and thermodynamics of compressible fluid flow, Vol. 1*. Ronald Press, New York, 1953.